THE ASTROPHYSICAL JOURNAL, 454:L35–L38, 1995 November 20

A FAR-ULTRAVIOLET SPECTRUM OF THE PUPPIS A SUPERNOVA REMNANT USING THE HOPKINS ULTRAVIOLET TELESCOPE

WILLIAM P. BLAIR[1]
Department of Physics and Astronomy, The Johns Hopkins University, 34th and Charles Streets, Baltimore, MD 21218; wpb@pha.jhu.edu
JOHN C. RAYMOND[2]
Smithsonian Astrophysical Observatory, 60 Garden Street, Cambridge, MA 02138; raymond@cfa.harvard.edu
KNOX S. LONG[1]
Space Telescope Science Institute, 3700 San Martin Drive, Baltimore, MD 21218; long@stsci.edu
AND
GERARD A. KRISS
Department of Physics and Astronomy, The Johns Hopkins University, 34th and Charles Streets, Baltimore, MD 21218; gak@pha.jhu.edu
Received 1995 July 3; accepted 1995 September 5

ABSTRACT

We report the first successful far-ultraviolet spectroscopic observation of a filament in the Puppis A supernova remnant. We observed a position on the eastern side of the remnant near the brightest X-ray region using the Hopkins Ultraviolet Telescope during the Astro-2 space shuttle mission in 1995 March. The spectrum covers the 820–1840 Å spectral range with ~3 Å resolution and shows numerous lines of C, N, O, Ne, He, and possibly Si. Comparison of this spectrum to solar abundance shock models indicates a shock velocity of approximately 160–180 km s^{-1}. A slight overabundance of N is possible for this position, consistent with a shocked interstellar medium picture for the observed filament. This is at odds with the much larger overabundance of N indicated by optical data from other regions of the outer shell in Puppis A. Comparison with optical CCD images obtained at Las Campanas Observatory and with *Einstein* HRI data indicates that the region observed corresponds to a very recent encounter between the blast wave and an interstellar cloud. The interaction of the shock wave with this cloud is responsible for the bright X-ray emission in this region.

Subject headings: ISM: individual (Puppis A) — ISM: supernova remnants — shock waves — ultraviolet: ISM

1. INTRODUCTION

Ultraviolet spectroscopic observations of supernova remnants (SNRs) provide unique knowledge about shock velocities, chemical abundances, and physical conditions in the material encountered by the SNR blast waves. However, Galactic SNRs are very concentrated toward the plane of the Galaxy, and all but a few are unobservable in the ultraviolet because of extinction. The Cygnus Loop and Vela SNRs are notable exceptions, with observations from the *International Ultraviolet Explorer* (*IUE*) satellite and even the *Voyager* Ultraviolet Spectrometers at a number of positions within their filamentary structures (Raymond et al. 1988; Raymond, Wallerstein, & Balick 1991; Blair et al. 1991a; Vancura et al. 1993; Hester, Raymond, & Blair 1994; Blair, Vancura, & Long 1995, and references therein). The Crab Nebula has been detected with *IUE* even though the reddening is high [$E(B-V) = 0.5$; see Davidson et al. 1982; Blair et al. 1992]. A handful of other Galactic remnants have been attempted with *IUE* without much success. Among these objects is the Galactic remnant Puppis A.

Puppis A is a very interesting SNR because it shows some signs of relative youth while also having a substantial physical extent and well-developed shell structure more characteristic of an evolved remnant. Arendt et al. (1990) show a multiwavelength morphological comparison of the emissions from, or associated with, Puppis A. In radio and X-ray images, the remnant appears as a nonuniform bubble, much brighter on the eastern side, with an angular extent of ~55′. Recent observations with *ROSAT* (Aschenbach 1993) have shown that the X-ray emission is harder in a band cutting across the middle of Puppis A from the NE to the SW, because of foreground absorption by the outermost shell of the Vela SNR. Distance estimates to Puppis A are typically in the range from 1.5–2.5 kpc (see Caswell & Lerche 1979; Dubner & Arnal 1988; Reynoso et al. 1995). Assuming 2 kpc, the physical diameter of the outer shell is 32 pc.

Optical spectra of some of the brighter outlying filaments have shown evidence for enhanced nitrogen abundances (Dopita, Mathewson, & Ford 1977; Winkler & Kirshner 1985), perhaps indicative of pre-SN mass loss from a massive star. This is consistent with the discovery of some oxygen-rich material seen near the center of Puppis A (Winkler & Kirshner 1985; Winkler et al. 1989), since such material is expected in the ejecta of supernovae from massive stars (see Woosley & Weaver 1986). However, proper motion studies of this O-rich material (Winkler et al. 1988) indicate an expansion age of only 3700 yr (assuming no deceleration); if this age is appropriate for the outer structure, it indicates an uncomfortably large mean expansion expansion velocity of 3200 km s^{-1}. While age estimates from Sedov models and age-diameter relationships are of order 4000–8000 yr (see Culhane 1977; Caswell & Lerche 1979), it is not clear that such estimates are appropriate for the nonuniform shell of Puppis A. No X-ray or radio enhancement is seen at the position of the O-rich

[1] Guest Observer, Las Campanas Observatory, operated by the Carnegie Institution of Washington.
[2] Astro-2 Guest Investigator.

material; it is possible that this material is expanding into a cavity produced by an earlier explosion, pointing to a multiple SN picture for Puppis A. Becker et al. (1995) have recently confirmed the presence of an X-ray point source in Puppis A using *ROSAT* observations.

The X-ray emission from Puppis A is dominated by a region of emission on the eastern side of the outer shell (Petre et al. 1982). Lucke et al. (1979), Clark et al. (1979), and Teske & Petre (1987) have observed this region in the optical coronal lines of iron, and develop a consistent picture involving a shocked interstellar cloud at this general position. We have used the Hopkins Ultraviolet Telescope (HUT) on the Astro-2 space shuttle mission to obtain a far-ultraviolet spectrum of a filament in this region of Puppis A. These are the first data to characterize the ultraviolet spectrum of Puppis A, and in particular they include coverage below Lyα down to the Lyman limit at 912 Å. We also show CCD/interference filter imagery of the region and the archival *Einstein* HRI data for comparison.

2. OBSERVATIONS AND REDUCTIONS

2.1. *Hopkins Ultraviolet Telescope Observations*

The HUT far-ultraviolet spectral observations were made during the Astro-2 space shuttle mission on 1995 March 12. HUT is a 0.9 m telescope that feeds an $f/2$ beam to a prime-focus spectrograph with a microchannel-plate image intensifier and a Reticon diode array detector. HUT was used to observe the 820–1840 Å spectral region with a resolution of $\sim 3 \pm 1$ Å. It operated from the shuttle as an attached payload, with scientists on the shuttle and at Spacelab Mission Operations Control at NASA/MSFC in Huntsville, Alabama, involved in performing the observations. The basic design and functionality of HUT are described by Davidsen et al. (1992). New optical coatings and other improvements made the Astro-2 version of HUT about 2.3 times more sensitive (Kruk et al. 1995).

The Puppis A observation used a $10'' \times 56''$ aperture positioned with its long dimension at position angle 135°. The position selected for observation, R.A.(1950) = $8^h22^m35^s.2$, decl. (1950) = $-42°47'53''.5$, corresponds to a linear [O III]-bright filament that approximately filled the aperture, as shown in Figure 1 (Plate L3). (This image will be discussed in the next section.) The filament was chosen because it appears to represent a single physical structure and it nearly filled the aperture, maximizing throughput. (The HUT detector does not provide spatial resolution within the aperture.) The aperture was positioned by aligning preplanned guide stars with fiducial marks placed on the HUT guide TV by the telescope's Dedicated Experiment Processor. Setup occurred during daylight, and the observation then proceeded throughout orbital night, where airglow emissions are at a minimum. We have extracted 1920 s of data that corresponded to the orbital night portion of the observation. Analysis of the pointing errors for the guide stars indicates that rms pointing remained stable to within 2″ during the observation.

The data reductions were performed in IRAF[3] using a modified package of tasks that was originally developed to process HUT data from Astro-1. At the time of this writing, a preliminary implementation of calibration and instrument performance data from Astro-2 is in place and was used to process these data (Kruk et al. 1995). The flux calibration applied to these data is based on in-orbit observations of white dwarf stars that have been fitted with theoretical models, and should be accurate to within 5% across the entire wavelength range. Other corrections, such as pulse persistence, dark count, and scattering properties, etc., have all been characterized to first order and included here, although improvements may still be forthcoming. Uncertainties in reddening correction (discussed below) are larger than any of these minor corrections.

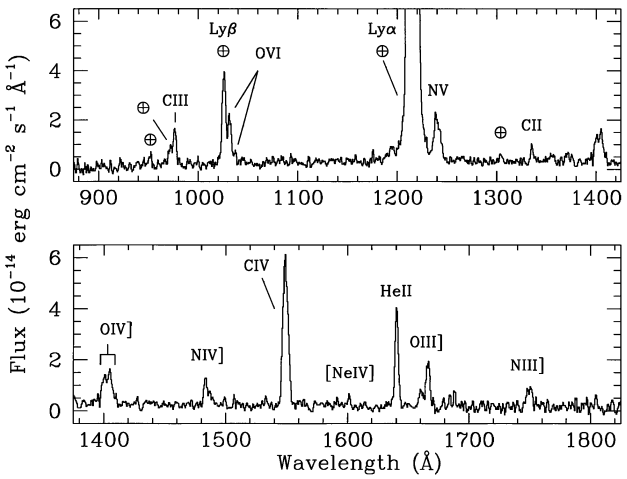

FIG. 2.—Observed, flux-calibrated HUT spectrum of the Puppis A SNR filament described in the text. Identifications for the major emission lines are shown, including several residual airglow emissions (marked with an Earth symbol).

The flux-calibrated HUT spectrum of Puppis A is shown in Figure 2. Below 1200 Å, O VI is clearly seen adjacent to the Lyβ airglow line, and C III is also observed adjacent to Lyγ. At longer wavelengths, many of the lines seen previously in other SNRs (see Blair et al. 1991b, and references therein) are detected for the first time in Puppis A. Even faint lines such as [Ne IV]λ1602 are detected at a low level. We have used the "deblend" function in the IRAF task "splot" to measure the integrated line fluxes, which are shown in Table 1 and scaled relative to F(C IV) = 100. The broad feature near 1400 Å is mainly O IV]; the Si IV line often seen at 1393 Å is weak or absent, and only an upper limit is shown in Table 1.

The reddening to Puppis A is moderately high and variable with position. Winkler & Kirshner (1985) adopt $E(B-V) = 0.5$ as representative for several filaments but do not provide explicit positions. Likewise, Dopita et al. (1977) list one Puppis A spectrum without noting its location; this spectrum appears to be consistent with a much lower reddening near $E(B-V) = 0.2$. We have unpublished long-slit optical spectra of a position south of the HUT aperture, cutting across the cloud core, obtained at Las Campanas. Using the hydrogen Balmer Hα:Hβ ratio in these data, a theoretical ratio of 3.0 (including a small collisional contribution to the ratio), and a Seaton (1979) curve, we find that $E(B-V)$ varies from 0.36–0.75 along the slit. The extinction to the filament observed with HUT is not known directly, and in such conditions of variable extinction, there is a tendency for the UV emission to come from regions of lower than average extinction. In

[3] IRAF is distributed by the National Optical Astronomy Observatories, which is operated by the Association of Universities for Research in Astronomy, Inc., (AURA) under cooperative agreement with the National Science Foundation.

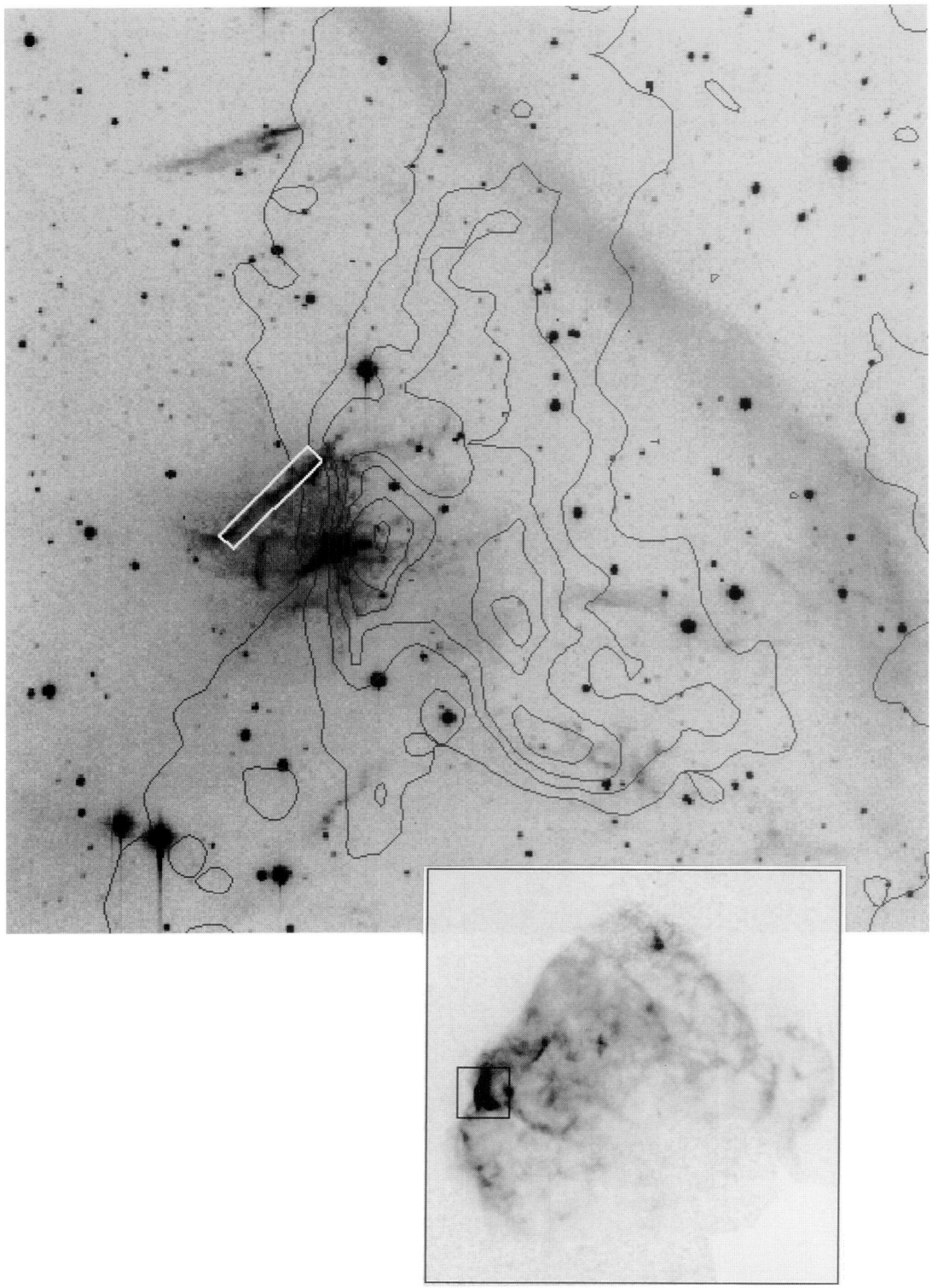

FIG. 1.—An optical [O III] CCD/interference filter image of the eastern cloud in Puppis A, obtained at Las Campanas Observatory. The inset shows the full (~57′) *Einstein* X-ray image, and the region shown in the optical image is highlighted as a box. The reconstructed position of the HUT 10″ × 56″ aperture is shown in the main figure by a white rectangle, and smoothed X-ray HRI contours of the region are also shown for reference.

BLAIR et al. (see 454, L36)

TABLE 1

PUPPIS A FAR-ULTRAVIOLET EMISSION LINE INTENSITIES COMPARED WITH MODELS

λ (Å)	Line ID	F_{obs}[a]	F(C IV=100)	I(0.2)[b]	I(0.5)[c]	I(V=160)[d]	I(V=180)[d]	I(CL)[e]
977	C III	5.9	19.7	60.3	352	61.1	72.8	69.2
991	N III	1.3:	4.3:	13.6:	77:	16.2	12.3	43.7
1025	Lyβa/g[f]	17.0	...	...	...	...	...	...
1032	O VI	8.4	...	...	...	...	...	...
1038	O VI	1.8	...	...	...	...	...	...
1035	$O\ VI_{tot}$[g]	13.0	42.0	90.4	325	52.5	434	198
1085	He II + [N II]	<0.8	<3	<7.5	<20	...	...	7.0
1240	N V	13.0	43.3	57.9	84.4	57.4	58.3	64.0
1335	C II	2.0	6.7	7.0	9.9	17.8	20.3	9.5
1371	O V	<1.5	<5.2	<5.5	<5.9	...	...	19.0
1393	Si IV	<1.5	<5.2	<5.5	<5.9	5.2	5.7	20.9
1404	O IV]	12.0	40.0	42.3	44.4	39.0	42.1	123
1486	N IV]	4.7	15.9	16.4	17	8.9	5.4	28.1
1549	C IV	30.0	100	100	100	100	100	100
1602	[Ne IV]	1.0:	3.4:	3.2:	2.8:	2.8	3.6	12.0
1640	He II	12.0	42.0	39.8	37.0	6.5	5.6	59.4
1661	O III]	2.5	8.3	...	...	...	...	...
1666	O III]	7.0	23.3	...	...	...	...	...
1664	$O\ III]_{tot}$	9.5	31.6	26.8	24.8	22.9	23.4	88.5
1749	N III]	4.4	14.7	13.4	12.5	6.4	5.3	27.0

[a] Observed fluxes are given in units of 10^{-14} ergs cm^{-2} s^{-1}.

[b] Reddening correction assuming $E(B-V) = 0.2$ and a standard galactic extinction curve (see text). For scaling, the reddening corrected C IV intensity is 1.3×10^{-12}: ergs cm^{-2} s^{-1}.

[c] Reddening correction assuming $E(B-V) = 0.5$ and a standard galactic extinction curve (see text). For scaling, the reddening corrected C IV intensity is 1.3×10^{-11} ergs cm^{-2} s^{-1}.

[d] Models shown are steady flow "E-series" models from Hartigan et al. 1987 for the velocities indicated.

[e] Reddening-corrected Cygnus Loop line intensities from Blair et al. 1991b.

[f] The strength of the Lyβ airglow line is shown for reference.

[g] O VI total corrected for molecular H absorption of λ1038 assuming a 2:1 ratio for the doublet.

Table 1 we list corrected line intensities for both $E(B-V) = 0.2$ and $E(B-V) = 0.5$ using a Galactic curve described by Longo et al. (1989), to make an approximate correction to relative line intensities for comparison with shock models. Scaling is again made relative to C IV = 100.

With such substantial extinction one might expect H_2 absorption in the region below 1108 Å (see Bowers et al. 1995). An indication of this may be the large observed ratio of O VI λλ1032, 1038, since H_2 absorption selectively affects the 1038 Å component. These lines normally appear in a 2:1 ratio, or less if optical depth is important (see Long et al. 1992). In Table 1 we list a total O VI intensity assuming 1.5 times the measured 1032 Å flux.

2.2. *CCD/Interference Filter Imagery and Einstein Data*

CCD/interference filter imagery was obtained at Las Campanas Observatory in Chile as part of a survey of southern Galactic SNRs. These data were obtained in 1987 April using the Swope 1 m telescope, a focal reducer, and an 800 × 800 pixel TI CCD. Details of the observational setup, filters, and the reductions have been described by Long, Blair, & van den Bergh (1988). Observations were obtained with filters that isolated the emission from Hα + [N II], [S II] λ6725, and [O III] λ5007. The full field of view at the 1 m was 14.′5 with 1.″1 pixels, but here we extract a 7′ subset of these data centered on the brightest X-ray emission. (The inset in Fig. 1 shows the location of the optical field.) After bias subtraction and flat-fielding, the subimages have been aligned to the nearest pixel. These images are shown in Figures 3*a*, 3*b*, and 3*c* (Plate L4).

For comparison to the optical data, we have obtained the *Einstein* X-ray data of Puppis A from the SAO *Einstein* CD-ROM. The full X-ray mosaic of Puppis A is shown as an inset on Figure 1. The radio morphology is similar to the X-ray, and an interaction with a molecular cloud on the eastern side of Puppis A is thought to be responsible for the remnant's observed morphology (Arendt et al. 1990; Reynoso et al. 1995). The HRI data for the region of interest were aligned with the optical images using the positions of *HST* Guide Star Catalog stars in the region and the coordinates in the header of the *Einstein* data. This alignment should be good to 4″. Independent confirmation of the alignment arises from comparison with the Teske & Petre (1987) [Fe XIV] optical image, which shows the stars in the region directly; the brightest HRI emission coincides with the bright [Fe XIV] emission. The aligned HRI data are shown in gray-tone format in Figure 3*d* and as contours overlaid on Figure 1, which is an enlarged version of the [O III] image. The X-ray emission is brightest on the back (west) side of the cloud, where an overpressure from an interaction with the cloud would be expected, and the X-rays can be seen wrapping around the cloud.

3. DISCUSSION

The ultraviolet spectrum reported above makes Puppis A only the fourth Galactic SNR for which FUV data are available, and only the third Galactic SNR to show O VI in emission (the others being the Cygnus Loop and Vela SNRs). In Table 1 we compare our spectrum of the Puppis A filament to steady flow/normal abundance shock models reported by Hartigan, Raymond, & Hartmann (1987, hereafter HRH). Two columns in Table 1 show the line strengths predicted by two "E-series" models from HRH, with shock velocities of 160 and 180 km s^{-1} scaled relative to a C IV λ1549 intensity of 100.

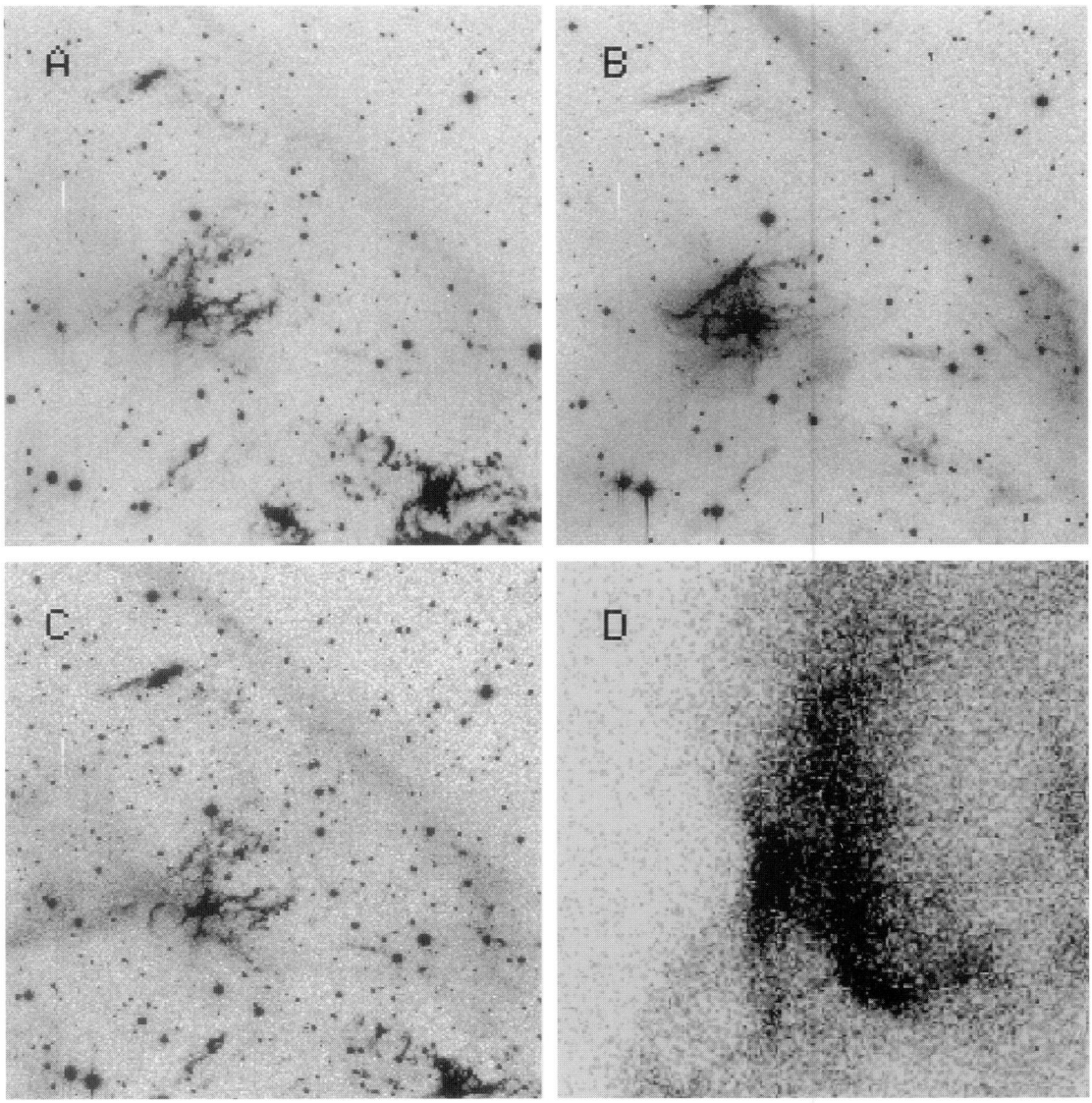

FIG. 3.—Las Campanas Observatory CCD/interference filter images of the eastern portion of the Puppis A SNR, and comparison to *Einstein* HRI data. (*a*) Hα + [N II] image; (*b*) [O III] λ5007 image; (*c*) [S II] λ6725 image; (*d*) *Einstein* HRI data in gray-tone format. North is up and east is to the left, and the region shown is 7′ on a side. Panel (*b*) is enlarged in Fig. 1.

These models were chosen because they bracket the range of O VI intensities predicted by the range of reddening corrections discussed above; O VI emission turns on near 160 km s^{-1} and increases in relative intensity very rapidly to 180 km s^{-1}.

Since we have scaled to C IV λ1549, the differential reddening effects are largest at the shortest wavelengths. If the reddening is as high as $E(B-V) = 0.5$, the C III λ977 line becomes very strong relative to C IV, with a value near that expected from models with $V = 100$ km s^{-1} (i.e., as the C IV line is just turning on with increasing shock velocity). The N III λ991 line shows much the same effect. This is at odds with the very large intrinsic C IV flux predicted by this same reddening correction (see footnotes to Table 1). Since O VI can only be produced by shocks with velocities higher than about 160 km s^{-1}, these arguments would seem to point to a lower value of the reddening at the observed position. Indeed, with the exception of O VI, most of the other strong lines change relative intensity very little between 160 and 180 km s^{-1} or between $E(B-V) = 0.2$ and 0.5.

Using the data corrected for $E(B-V) = 0.2$, we see encouraging agreement between the observed line intensities and those predicted for a velocity somewhat in excess of 160 km s^{-1}. The main differences are that He II λ1640 is much stronger than predicted by the models (a problem noticed previously in spectra of the Cygnus Loop—see below), and C II λ1335 is weaker than predicted by the models (again seen in other objects and often attributed to resonance scattering effects). Also, the various lines of nitrogen seem to be high by a factor of ~2 in relative intensity. This is not as extreme as the factor of 6 nitrogen enhancement inferred from optical spectra elsewhere in Puppis A (see Dopita et al. 1977). The fact that solar abundance models can roughly match the observed line intensities indicates the material at this location is mainly interstellar, rather than circumstellar, in origin. This is consistent with the picture whereby the shock wave is encountering a molecular cloud on the eastern side of Puppis A.

The last column in Table 1 shows reddening-corrected line intensities for a position in the Cygnus Loop observed with HUT during Astro-1 (Blair et al. 1991b). While the highest ionization lines in the Cygnus Loop spectrum are consistent with a shock velocity of ~170 km s^{-1}, lower ionization lines are much stronger than expected, implying a mixing of shock velocities within the aperture. This is consistent with the complex morphology of the region on images in various optical emission lines. With the exception of the N line strengths noted above, no such enhancement of low and intermediate ionization lines is seem in the Puppis A spectrum. While it is possible that the situation in Puppis A is more complex than a single steady flow shock, the basic agreement with a steady flow model and the linear, coherent appearance of the observed filament makes this picture tenable until more detailed observations become available.

The optical appearance of the region gives the strong impression that an interstellar cloud is being disrupted by its encounter with the blast wave (see Stone & Norman 1992; Klein, McKee, & Colella 1994). Although we cannot unravel projection effects without detailed velocity information, the X-ray data show clear correlation with the cloud. The X-rays are brightest on the western (back) side of the cloud and can be seen wrapping around it, with the leading edge of the X-ray emission north and south of the cloud correlating with ridges visible in the diffuse [O III] gas at these locations. The enhanced diffuse [O III] to the east from this position could indicate preshock photoionization, while the diffuse optical emission behind the X-ray shock front and enveloping the cloud itself may imply evaporation (see discussion by Teske & Petre 1987) and/or an overpressured reverse shock due to the primary shock's encounter with the cloud (see Hester & Cox 1986; Hester, Raymond, & Blair 1994).

It is puzzling that the observed filament (as well as much of the cloud) appears to be ahead of the X-ray emission, but the FUV spectrum leaves little doubt that the entire cloud has been enveloped by the blast wave. We can only assume that projection effects and differential absorption combine to cause the observed effect. We note that a small, roughly radial filament several arcminutes north of the cloud also extends ahead of the X-ray edge, and the bright Hα and [S II] filaments ~4′ SW of the cloud also show no correlation with X-ray emission (see Fig. 3). Future optical high- and low-resolution spectroscopy in conjunction with the data presented here will be needed to improve our understanding of this region of Puppis A.

The Astro-2 Space Shuttle mission was a resounding success, and we thank everyone involved, from mission management and support personnel at NASA/MSFC to the crew of *Endeavour* to our many colleagues on the HUT team at Johns Hopkins and the JHU Applied Physics Laboratory. W. P. B. thanks Richard Teske and Frank Winkler for previous discussions about Puppis A. This research is supported by NASA through contract NAS 5-27000 to the Johns Hopkins University.

REFERENCES

Arendt, R. G., Dwek, E., Petre, R., Dickel, J. R., Roger, R. S., Milne, D. K., & Kesteven, M. J. 1990, ApJ, 350, 266
Aschenbach, B. 1993, in UV and X-Ray Spectroscopy of Laboratory and Astrophysical Plasmas, ed. E. Silver & S. Kahn (Cambridge: Cambridge Univ. Press), 434
Becker, C. M., Petre, R., & Winkler, P. F. 1995, BAAS, 27, 864
Blair, W. P., Long, K. S., Vancura, O., & Holberg, J. B. 1991a, ApJ, 374, 202
Blair, W. P., et al. 1991b, ApJ, 379, L33
———. 1992, ApJ, 399, 611
Blair, W. P., Vancura, O., & Long, K. S. 1995, AJ, 110, 312
Bowers, C. W., et al. 1995, ApJ, 444, 748
Caswell, J. L., & Lerche, I. 1979, MNRAS, 187, 201
Clark, D. H., Murdin, P., Zarnecki, J. C., & Culhane, J. L. 1979, MNRAS, 188, 11P
Culhane, J. 1977, in Supernovae, ed. by D. N. Schramm (Dordrecht: Reidel), 29
Davidsen, A. F., et al. 1992, ApJ, 392, 264
Davidson, K., et al. 1982, ApJ, 253, 696
Dopita, M. A., Mathewson, D. S., & Ford, V. L. 1977, ApJ, 214, 179
Dubner, G. M., & Arnal, E. M. 1988, A&AS, 75, 363
Hartigan, P., Raymond, J., & Hartmann, L. 1987, ApJ, 316, 323 (HRH)
Hester, J. J., & Cox, D. 1986, ApJ, 300, 675
Hester, J. J., Raymond, J. C., & Blair, W. P. 1994, ApJ, 420, 721
Klein, R. I., McKee, C. F., & Colella, P. 1994, ApJ, 420, 213
Kruk, J. W., Durrance, S. T., Kriss, G. A., Davidsen, A. F., Blair, W. P., Espey, B. R., & Finley, D. 1995, ApJ, 454, L1
Long, K. S., Blair, W. P., & van den Bergh, S. 1988, ApJ, 333, 749
Long, K. S., et al. 1992, ApJ, 400, 214
Longo, R., Stalio, R., Polidan, R. S., & Rossi, L. 1989, ApJ, 339, 478
Lucke, R. L., Zarnecki, J. C., Woodgate, B. E., Culhane, J. L., & Socker, D. G. 1979, ApJ, 228, 763
Petre, R., Canizares, C. R., Kriss, G. A., & Winkler, P. F. 1982, ApJ, 258, 22
Raymond, J. C., Hester, J. J., Cox, D., Blair, W. P., Fesen, R. A., & Gull, T. R. 1988, ApJ, 324, 869
Raymond, J. C., Wallerstein, G., & Balick, B. 1991, ApJ, 383, 226
Reynoso, E. M., Dubner, G. M., Goss, W. M., & Arnal, E. M. 1995, AJ, 110, 318
Seaton, M. J. 1979, MNRAS, 187, 73P
Stone, J. M., & Norman, M. L. 1992, ApJ, 390, L17
Teske, R. G., & Petre, R. 1987, ApJ, 314, 673
Vancura, O., Blair, W. P., Raymond, J. C., & Holberg, J. B. 1993, ApJ, 417, 663
Winkler, P. F., & Kirshner, R. P. 1985, ApJ, 299, 981
Winkler, P. F., Kirshner, R. P., Hughes, J. P., & Heathcoat, S. R. 1989, Nature, 337, 48
Winkler, P. F., Tuttle, J. H., Kirshner, R. P., & Irwin, M. J. 1988, in IAU Colloq. 101, Supernova Remnants and the Interstellar Medium, ed. R. S. Roger & T. L. Landecker (Cambridge: Cambridge Univ. Press), 65
Woosley, S. E., & Weaver, T. A. 1986, ARA&A, 24, 205